

# Field test results for a 16-QAM and a 64-QAM digital radio, compared with the prediction based on sweep measurements

Autor(en): **Liniger, Markus / Vergeres, Daniel**

Objektyp: **Article**

Zeitschrift: **Technische Mitteilungen / Schweizerische Post-, Telefon- und Telegrafienbetriebe = Bulletin technique / Entreprise des postes, téléphones et télégraphes suisses = Bollettino tecnico / Azienda delle poste, dei telefoni e dei telegrafi svizzeri**

Band (Jahr): **64 (1986)**

Heft 7

PDF erstellt am: **10.07.2024**

Persistenter Link: <https://doi.org/10.5169/seals-875038>

## **Nutzungsbedingungen**

Die ETH-Bibliothek ist Anbieterin der digitalisierten Zeitschriften. Sie besitzt keine Urheberrechte an den Inhalten der Zeitschriften. Die Rechte liegen in der Regel bei den Herausgebern.

Die auf der Plattform e-periodica veröffentlichten Dokumente stehen für nicht-kommerzielle Zwecke in Lehre und Forschung sowie für die private Nutzung frei zur Verfügung. Einzelne Dateien oder Ausdrucke aus diesem Angebot können zusammen mit diesen Nutzungsbedingungen und den korrekten Herkunftsbezeichnungen weitergegeben werden.

Das Veröffentlichen von Bildern in Print- und Online-Publikationen ist nur mit vorheriger Genehmigung der Rechteinhaber erlaubt. Die systematische Speicherung von Teilen des elektronischen Angebots auf anderen Servern bedarf ebenfalls des schriftlichen Einverständnisses der Rechteinhaber.

## **Haftungsausschluss**

Alle Angaben erfolgen ohne Gewähr für Vollständigkeit oder Richtigkeit. Es wird keine Haftung übernommen für Schäden durch die Verwendung von Informationen aus diesem Online-Angebot oder durch das Fehlen von Informationen. Dies gilt auch für Inhalte Dritter, die über dieses Angebot zugänglich sind.

# Field test results for a 16-QAM and a 64-QAM digital radio, compared with the prediction based on sweep measurements

Markus LINIGER and Daniel VERGERES, Berne

## 1 Introduction

In 1980, the Swiss PTT started to measure the multipath transfer function on several hops of the national microwave radio relay network. Until now five hops have been investigated with a link analyzer sweeping over a bandwidth of 40 MHz or 60 MHz. The summary of the following results offers a comparison between different hops. Thus, it supplements the data published previously [1, 2]. In the most recent test run, which is still continuing, two additional digital radios are installed in order to measure the performance of the transmission at 140 Mbit/s. All of the following time-dependent statistics are valid for the worst month with a return-period of one year.

## 2 Description of the experiment

Since September 1985, the experiment (Fig. 1) has been in progress on one of the most unfavorable hops of the Swiss radio relay network. The 112 km La Dôle-Ulmizberg link (Fig. 5) was selected in order to reach the worst case of the possible multipath effect on digital radio in Switzerland. The two installed radios, one (NEC)

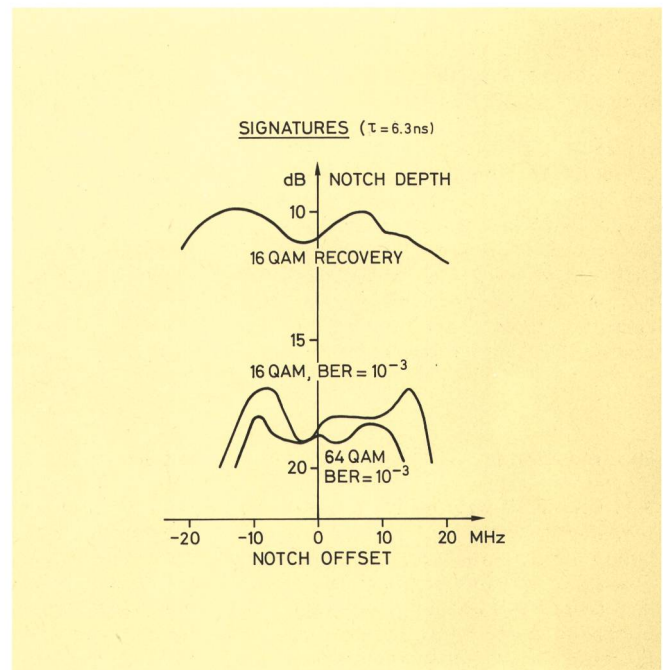


Fig. 2 Signatures of the digital radios

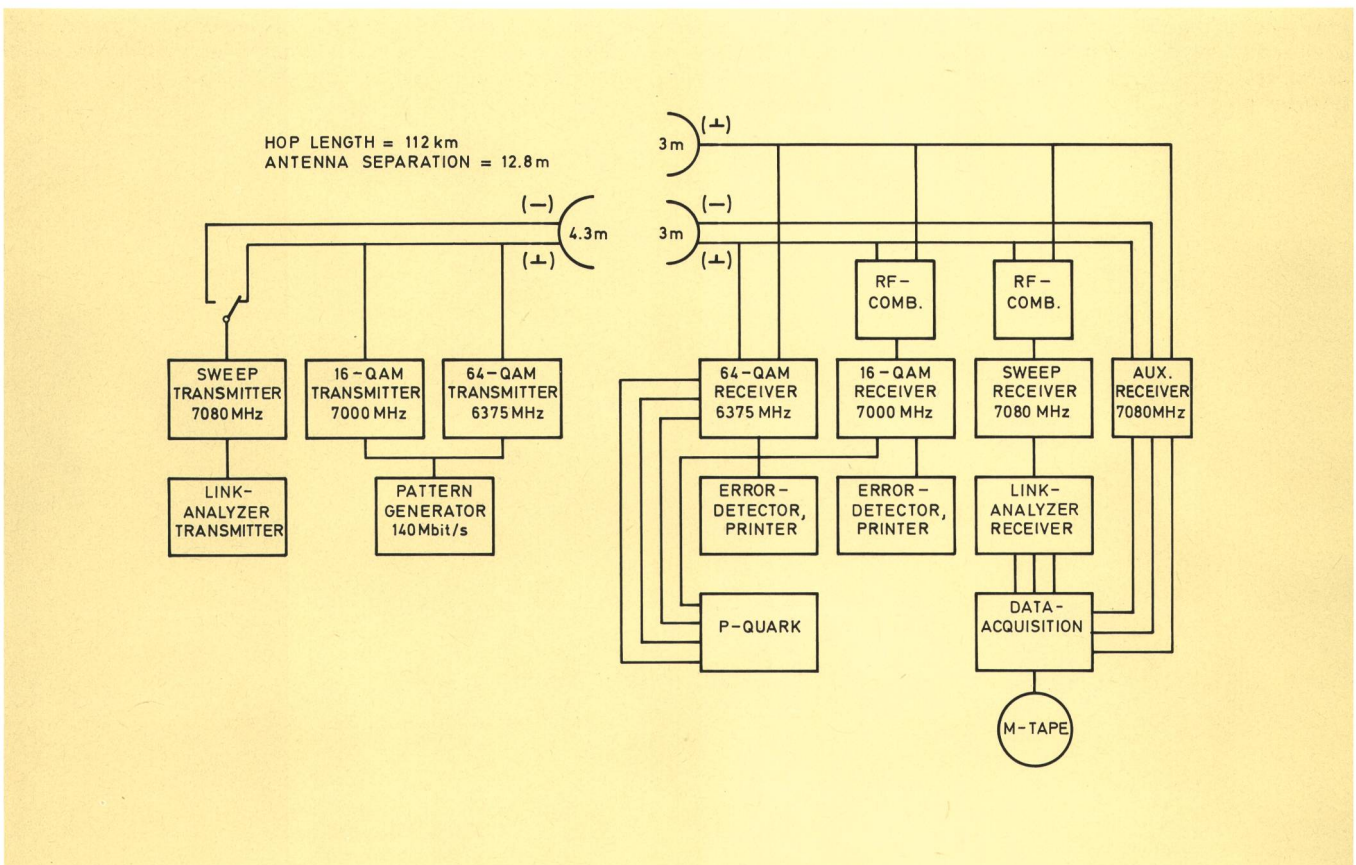


Fig. 1 Test configuration

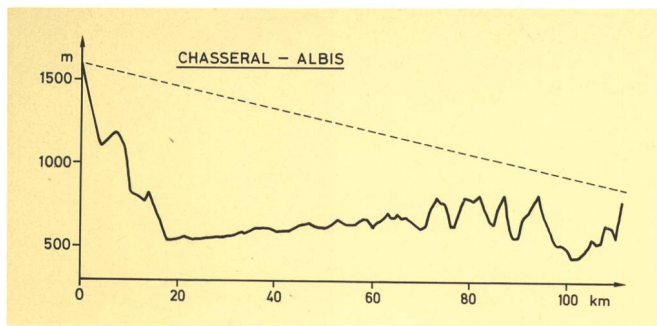


Fig. 3  
Path profile of the hop Chasseral-Albis

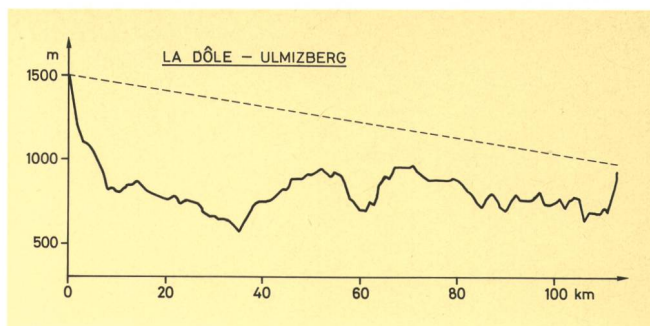


Fig. 5  
Path profile of the hop La Dôle-Ulmizberg

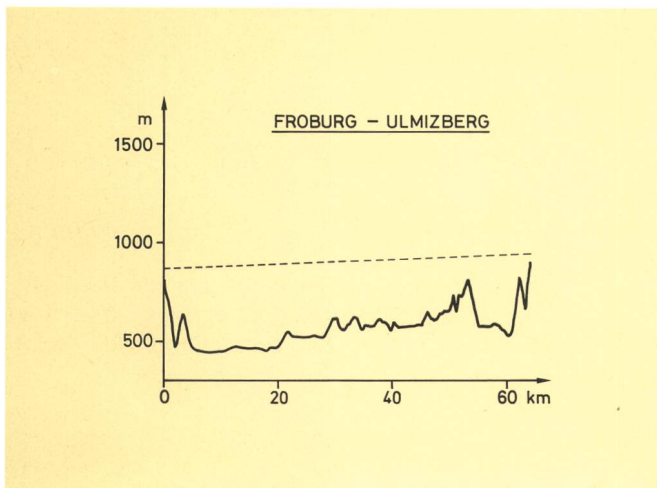


Fig. 4  
Path profile of the hop Froburg-Ulmizberg

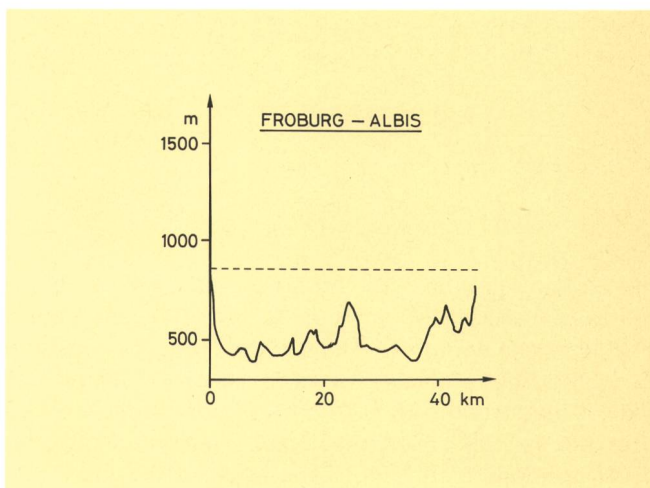


Fig. 6  
Path profile of the hop Froburg-Albis

using 16-QAM modulation and one (NT) 64-QAM, transmit 140 MBit/s. The signatures and the bit error performance of the radios are given in *Figures 2 and 9*. The

test of the two equipment in the same environment should allow a comparison under real multipath conditions. Both radios receive the signals from the main and

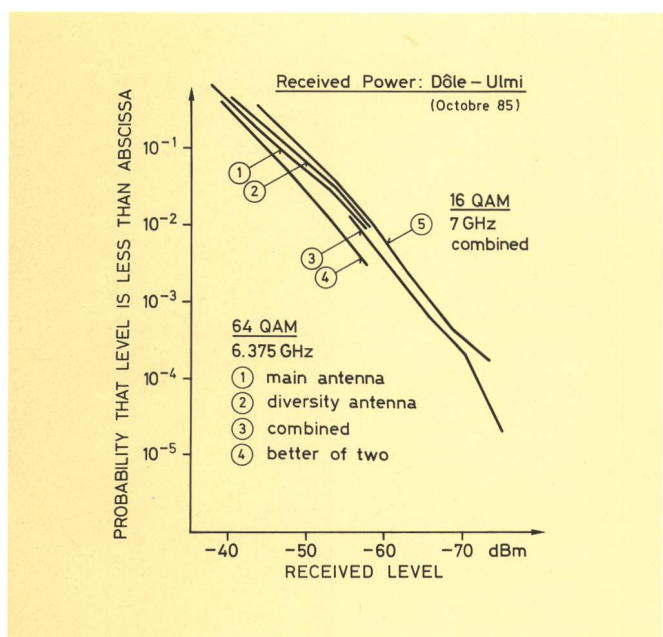


Fig. 7  
Measured cumulative distributions of the received power  
(October 1985)

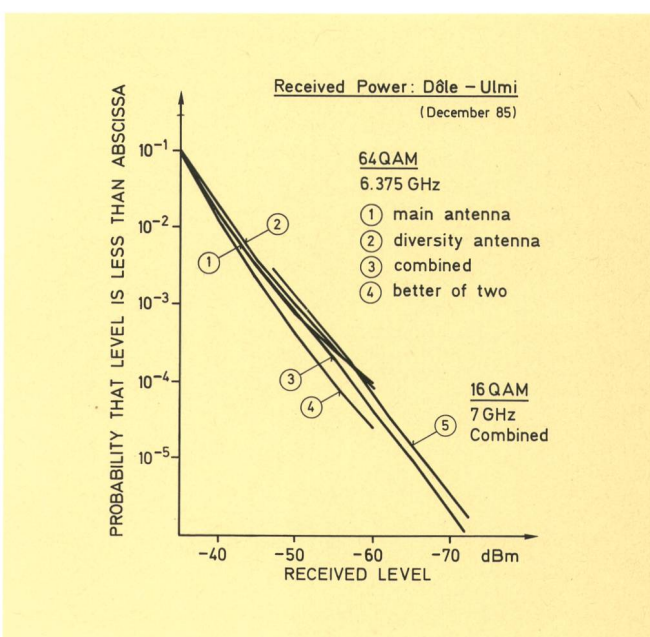


Fig. 8  
Measured cumulative distributions of the received power  
(December 1985)

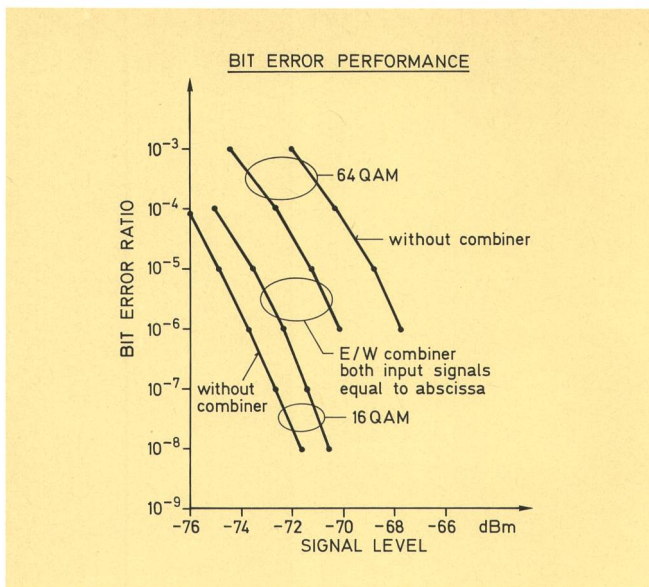


Fig. 9  
Bit error performance of the digital radios

the auxiliary antenna. The 16-QAM radio has an RF in-phase combiner (STR) and the 64-QAM one uses a built-in IF in-phase combiner. The bit error ratio is measured in one second intervals. The received power of the two radios is recorded with a P-QARK (programmable quantizer analyzer and record keeper), an equipment specially developed from Bell Labs for field tests. The results are given in *Figures 7, 8 and 32*.

The distortions occurring on this hop are measured using a link analyzer sweeping over a bandwidth of 60 MHz. The RF signal is transmitted by a parabolic antenna (4.3 m  $\phi$ ) alternately on both polarizations. At the receiver site two parabolic antennas were installed (3 m  $\phi$ ) with a vertical separation of 12.8 m. The magnitude of the three receive signals are fed to the data acquisition

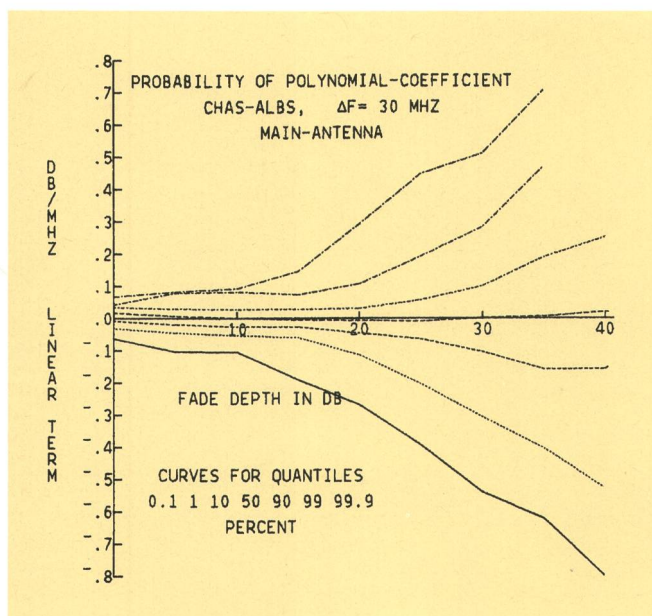


Fig. 10  
Probability of the amplitude slope dispersion, main-antenna

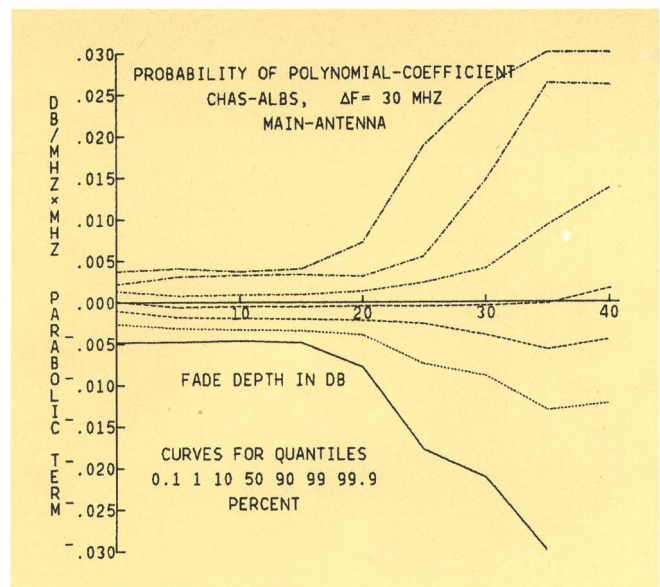


Fig. 11  
Probability of the amplitude parabolic dispersion, main-antenna

system. The two vertically polarized signals are combined through an in-phase diversity combiner. Its output is analyzed with a link analyzer and also fed to the computer.

### 3 Description of the investigated hops

Within the last six years the sweep experiment has been run on three other hops. They supplied sufficient measured fading data which allows a description of their behaviour under multipath conditions.

The 111 km Chasseral-Albis link (*Fig. 3*) was investigated from March 1981 to February 1982 sweeping in a 40 MHz channel of the 11 GHz band. The data base consists of

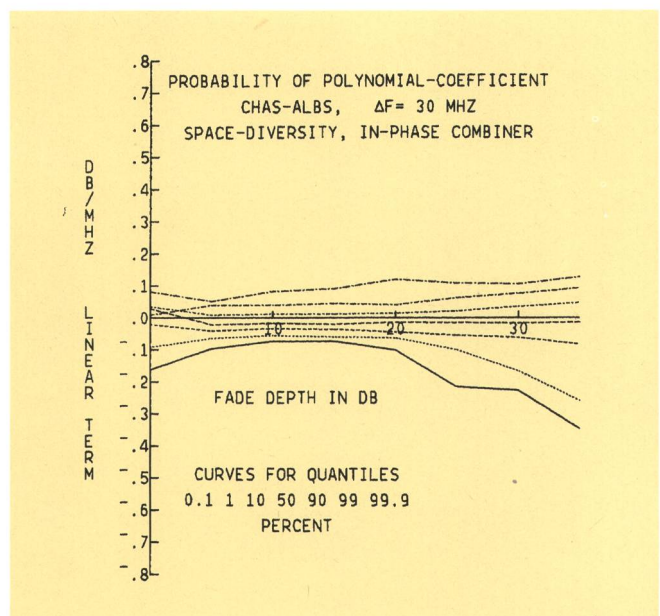


Fig. 12  
Probability of the amplitude slope dispersion, space diversity - in-phase combiner

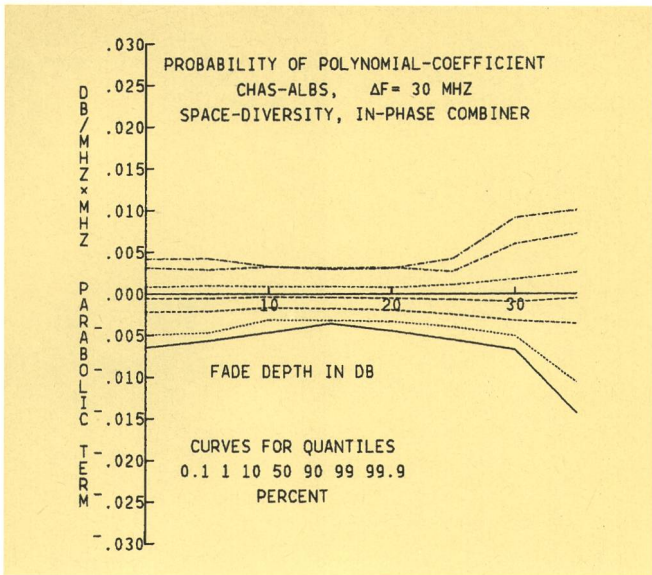


Fig. 13  
Probability of the amplitude parabolic dispersion, space diversity – in-phase combiner

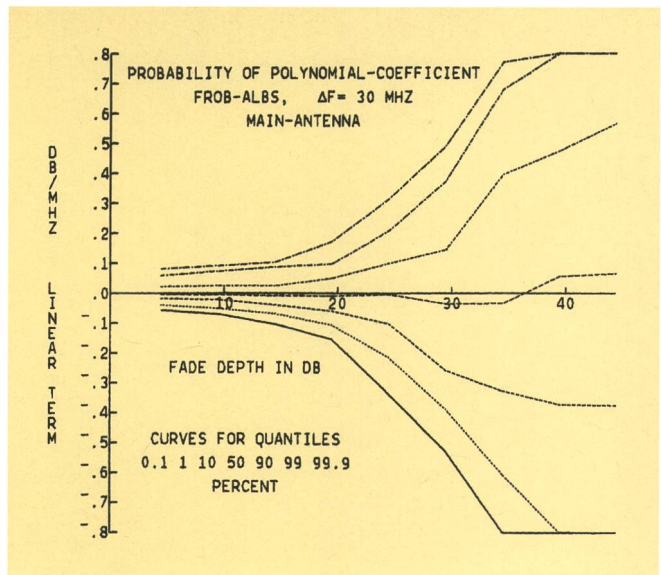


Fig. 16  
Probability of the amplitude slope dispersion, main-antenna

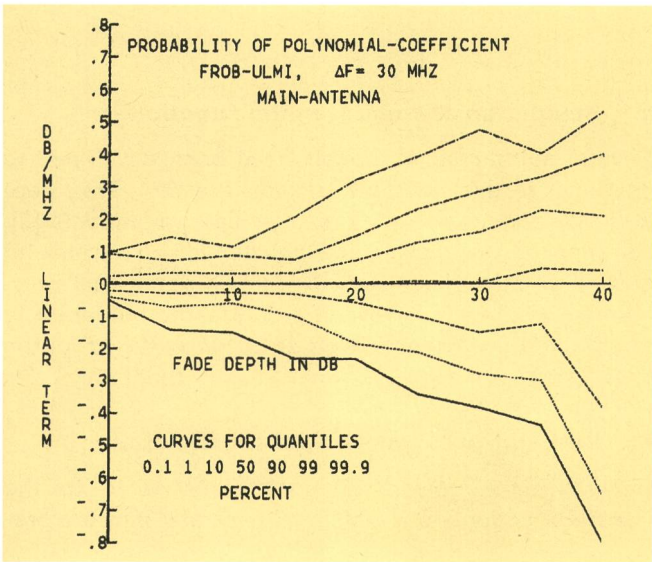


Fig. 14  
Probability of the amplitude slope dispersion, main-antenna

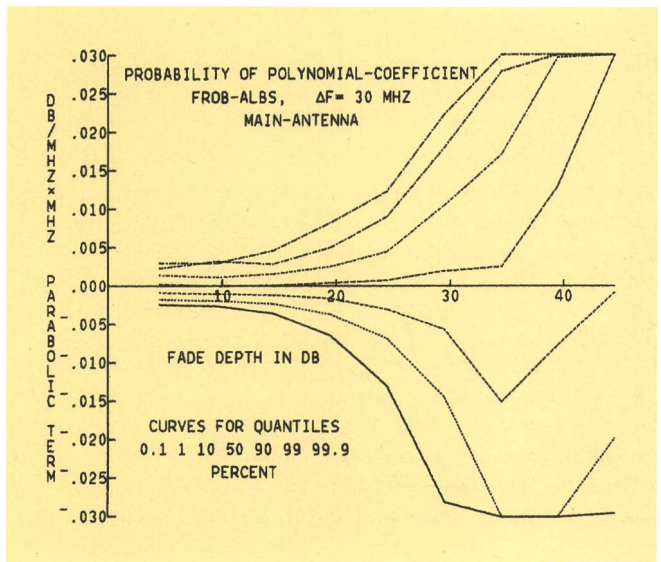


Fig. 17  
Probability of the amplitude parabolic dispersion, main-antenna

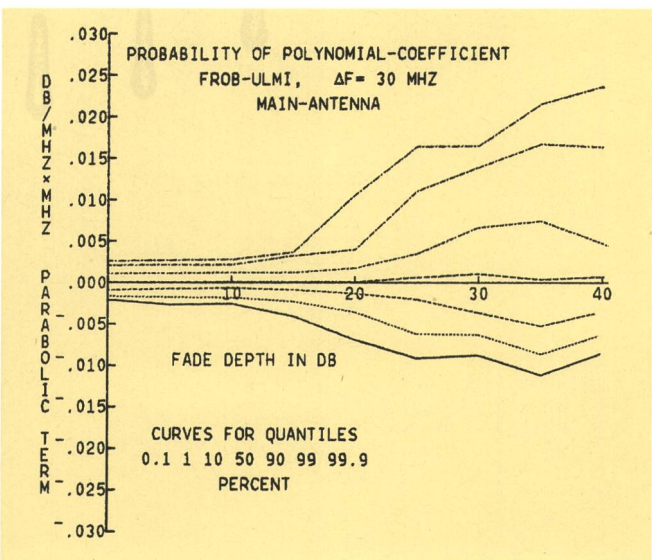


Fig. 15  
Probability of the amplitude parabolic dispersion, main-antenna

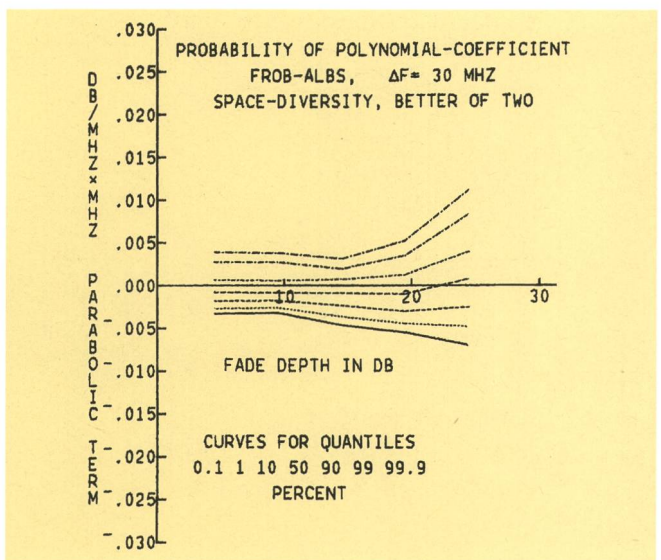


Fig. 18  
Probability of the amplitude slope dispersion, space diversity – better of two

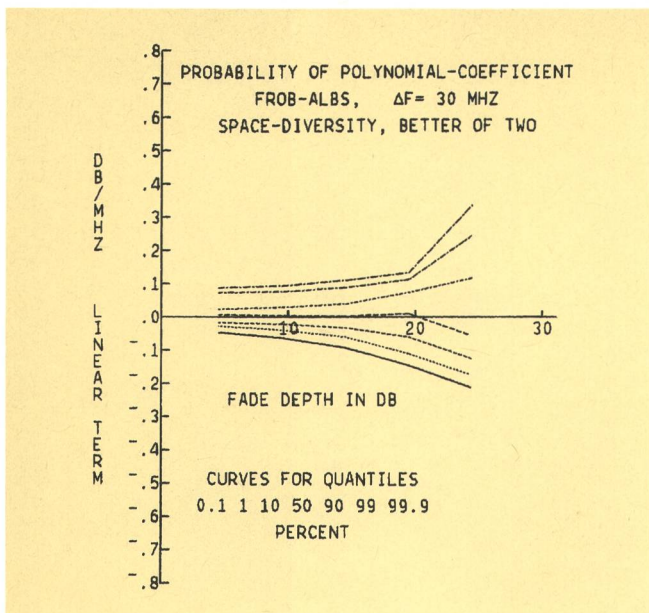


Fig. 19  
Probability of the amplitude parabolic dispersion, space diversity - better of two

about 2.5 million sweeps measured with and without space-diversity [1].

The 64 km Froburg-Ulmizberg link (Fig. 4) was under test between March 1982 and August 1983 (7 GHz, 60 MHz sweep, 0.5 million sweeps).

The 46 km Froburg-Albis link (Fig. 6) was studied with an improved test set-up, similar to that given in Figure 1, from September 1983 to April 1985 (7 GHz, 60 MHz sweep, switched polarizations, 2.5 million sweeps).

The 112 km La Dôle-Ulmizberg link (Fig. 5) test has been started in September 1985. The following results are based on a two-month period (0.4 million sweeps).

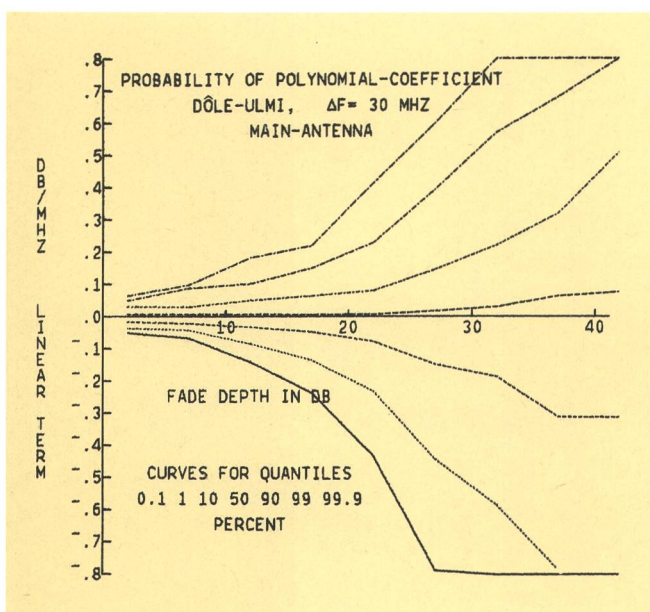


Fig. 20  
Probability of the amplitude slope dispersion, main-antenna

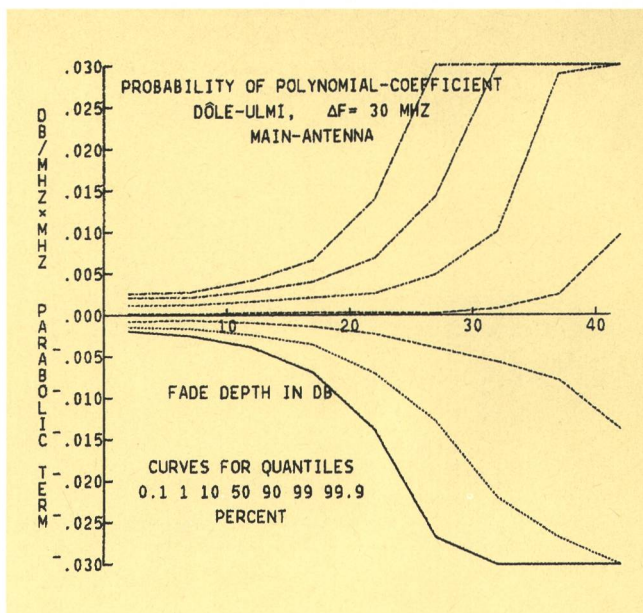


Fig. 21  
Probability of the amplitude parabolic dispersion, main-antenna

#### 4 Results on channel transfer function

Several mathematical models have been developed to characterize the multipath transfer function. They generally belong to one of three families: ray-models [3], complex- [4] respectively real polynomial-expansions [5] and parametric models [6, 7]. In this paper real polynomials of second order and a parametric model using the in-band-power-difference (IBPD) are applied for the characterization of the channel transfer function.

#### 4.1 Probability of polynomial coefficients

Generally, the polynomial coefficients fitted to the transfer function are correlated. Therefore, they are pre-

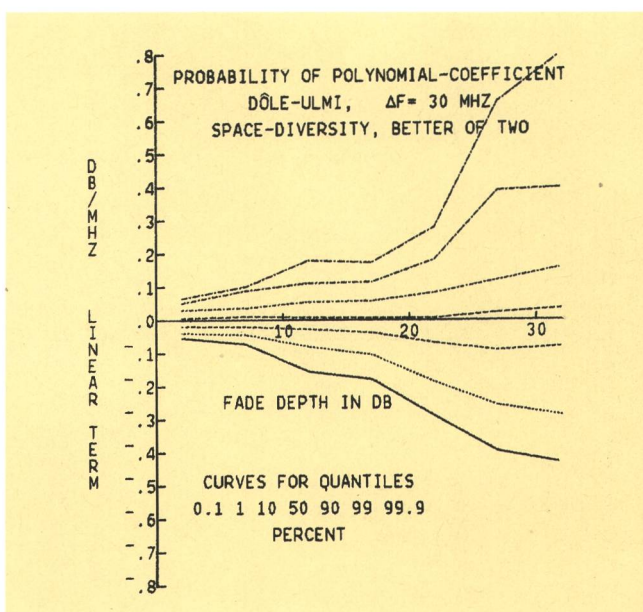


Fig. 22  
Probability of the amplitude slope dispersion, space diversity - better of two

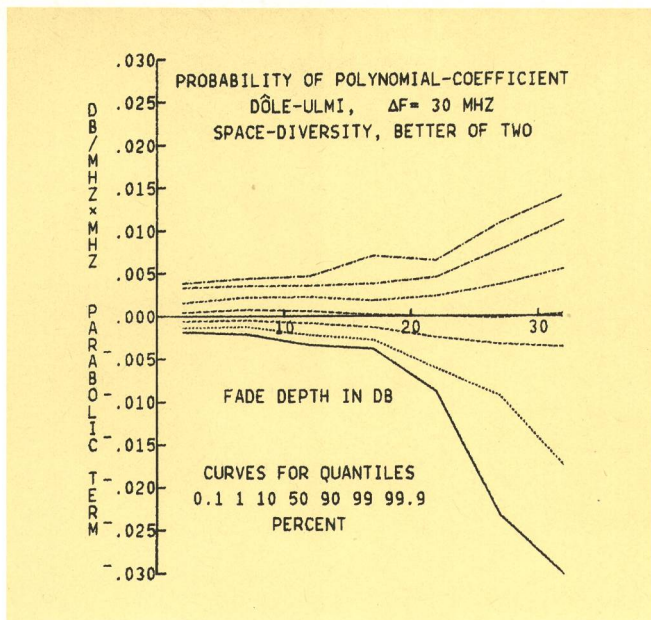


Fig. 23  
Probability of the amplitude parabolic dispersion, space diversity - better of two

sented with joint-probability distribution functions  $p(a_1, a_2/a_0)$  [1]. But for a comparison of the different hops it seems to be adequate to use only the marginal distributions  $p(a_1/a_0, \text{all } a_2)$  and  $p(a_2/a_0, \text{all } a_1)$ . Figures 10 to 23 show the quantiles (0.1, 1, 10, 50, 90, 99, 99.9 %) for the slope and parabolic distortion as a function of the fade depth. The Froburg-Ulmizberg hop is the one with the weakest distortions, La Dôle-Ulmizberg is the one with the strongest distortions. The probability that a given distortion occurs can be calculated as the product of the probability of the fade depth  $p(a_0)$  (Fig. 24 to 27) and the probability of the distortion at that fade depth. In addition, the remaining distortion with space-diversity reception is presented in Figures 12, 13, 18 and 19. All results are valid for a bandwidth of 30 MHz.

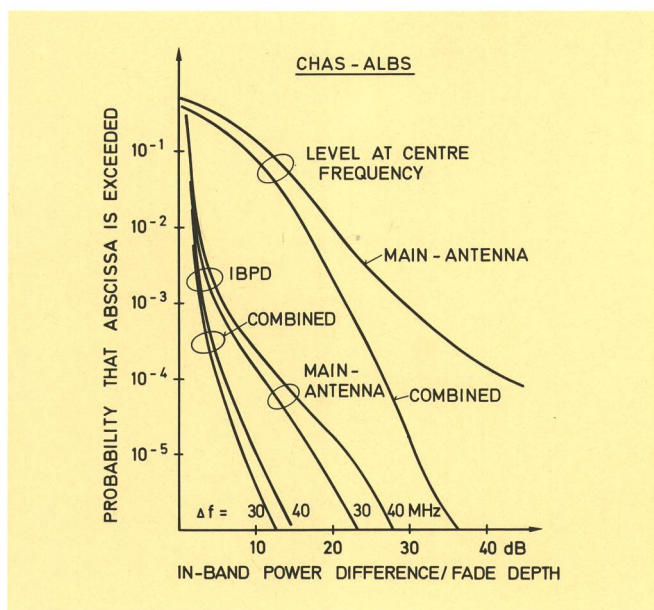


Fig. 24  
Measured cumulative distributions of amplitude dispersion (IBPD) or single frequency fade depth

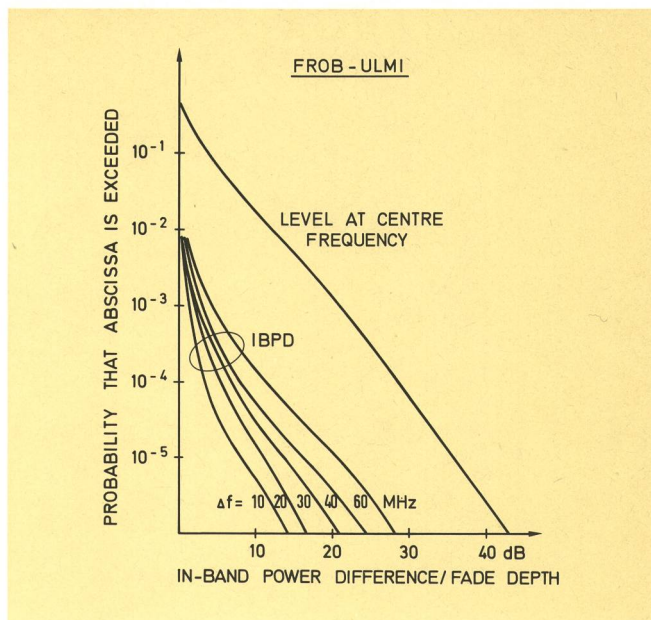


Fig. 25  
Measured cumulative distributions of amplitude dispersion (IBPD) or single frequency fade depth

#### 4.2 Probability of in-band-power-difference

The IBPD is the maximum difference of the received power in dB in a given frequency band and was calculated for different bandwidths (Fig. 24 to 27). It shows also the improvement gained by the space-diversity reception. The most unfavorable hop is again La Dôle-Ulmizberg.

#### 5 Estimated transmission performance

The transmission performance is determined by the flat and the dispersive fades. Using the method published in [1], the outage-probability is estimated as a function of

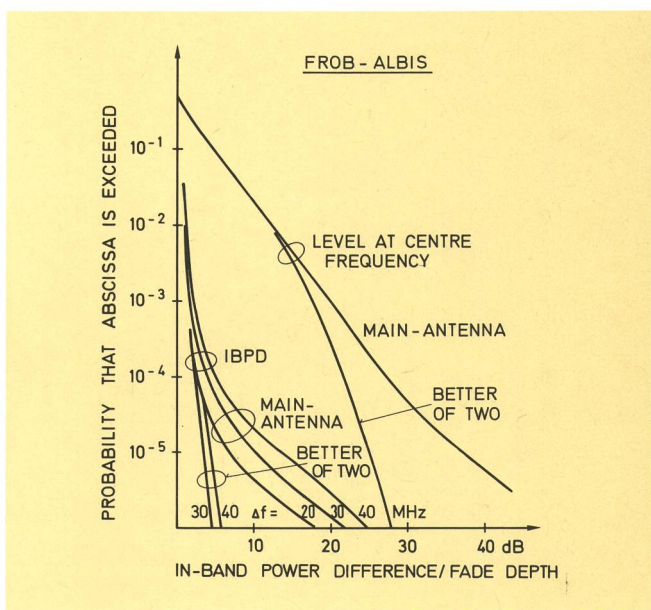


Fig. 26  
Measured cumulative distributions of amplitude dispersion (IBPD) or single frequency fade depth

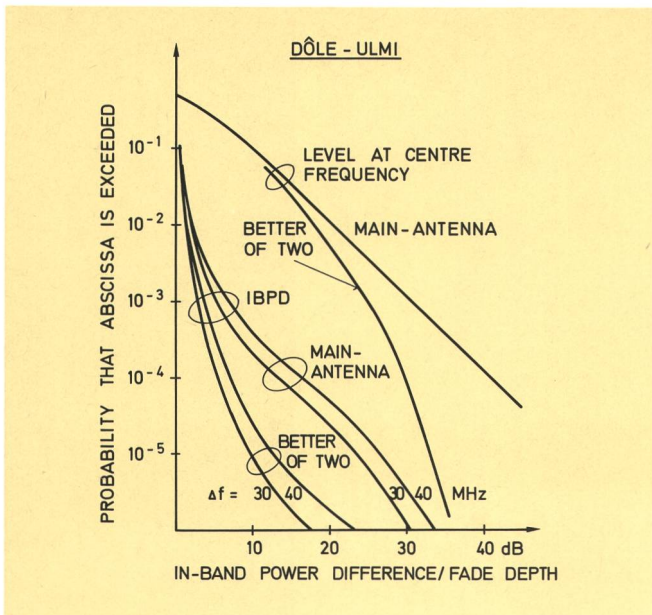


Fig. 27 Measured cumulative distributions of amplitude dispersion (IBPD) or single frequency fade depth

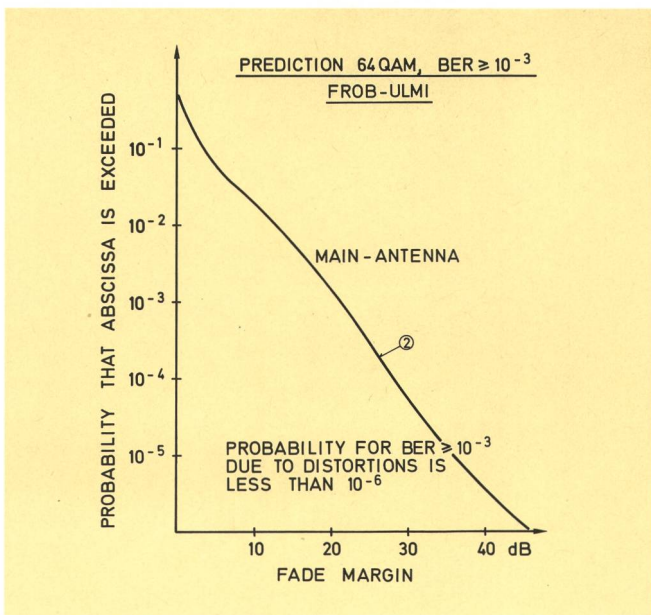


Fig. 29 Predicted outage probability based on measured distributions of fade depth and amplitude dispersion

the fade margin. With increasing fade margin, the effect of the dispersive fades increases (curve 1) and the one of the flat fades (curve 2) decreases (Fig. 28 to 31). The sum of both effects is described by the thick line. Curve 1 is plotted only for the 64-QAM radio, the values for the 16-QAM radio are about twice as high. Curve 2 is valid for both.

### 6 Measured transmission performance

From October to December 1985 we observed during a few hours events affecting the digital transmission. The measured bit error probabilities are plotted in Figure 32. The more sophisticated modulation scheme shows, con-

trary to initial expectation, the better performance. There are several reasons. First, the 16-QAM radio has 2 dB less transmit power. Second, the RF combiner increases more the noise figure of the receiver (and so decreases the flat fade margin) than the IF combiner. And third, the signature of the 16-QAM radio is much worse in case of recovery after loss of synchronization. The comparison of the time level below, the bit error performance of the equipment (Fig. 7, 8 and 9) and the measured bit errors leads to the conclusion that for the present configuration the flat fade effect dominates the dispersive fade. In the next test phase, the time level below caused by flat fades should be decreased by using an antenna separation of 19 m instead of 12.8 m.

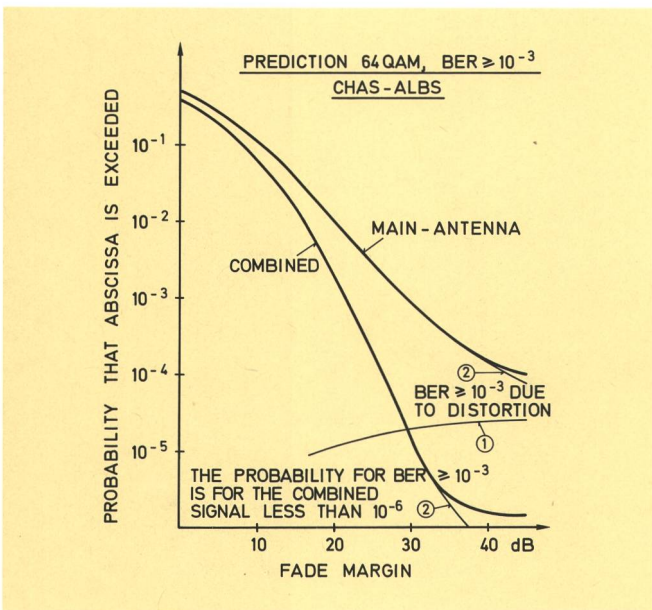


Fig. 28 Predicted outage probability based on measured distributions of fade depth and amplitude dispersion

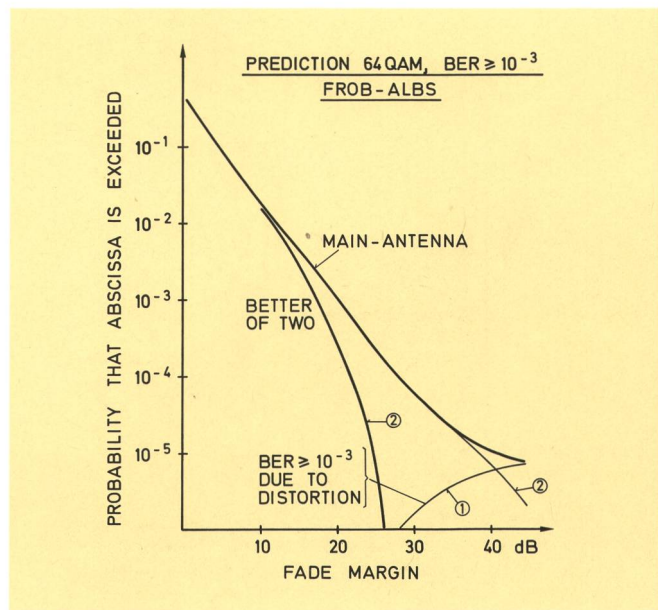


Fig. 30 Predicted outage probability based on measured distributions of fade depth and amplitude dispersion



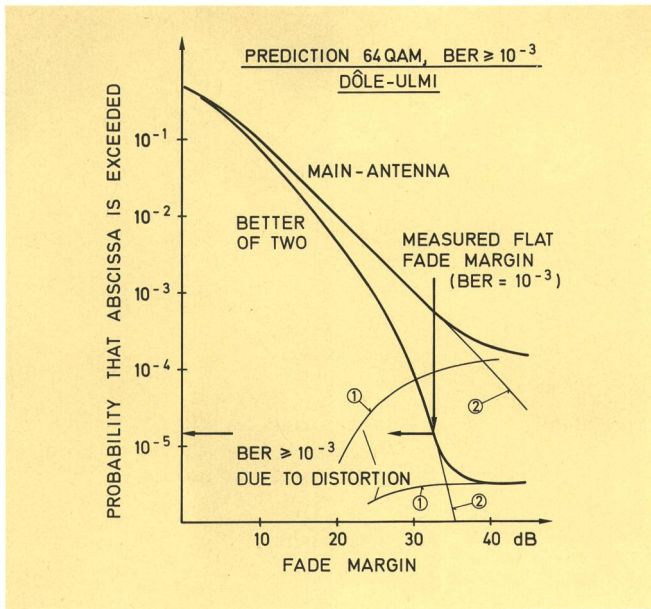


Fig. 31  
Predicted outage probability based on measured distributions of fade depth and amplitude dispersion

## 7 Conclusions

The experiment carried out on one of the most unfavorable hops in Switzerland has shown that a 16-QAM radio (augmented by a separate RF combiner, which could be improved by about 2 dB) and a 64-QAM radio (using a built-in IF combiner) show about the same performance. The outage time is, thanks to the good signatures, caused mainly by the flat fades. The estimated outage time, extracted from the results of the sweep experiment, shows good agreement with the measured one. Therefore, an extrapolation of the results to other hops of our radio relay network was made. It convinced us that an equipment with the same performance as the ones used can be applied on similar links and will meet the CCIR recommendation 594 (performance objectives).

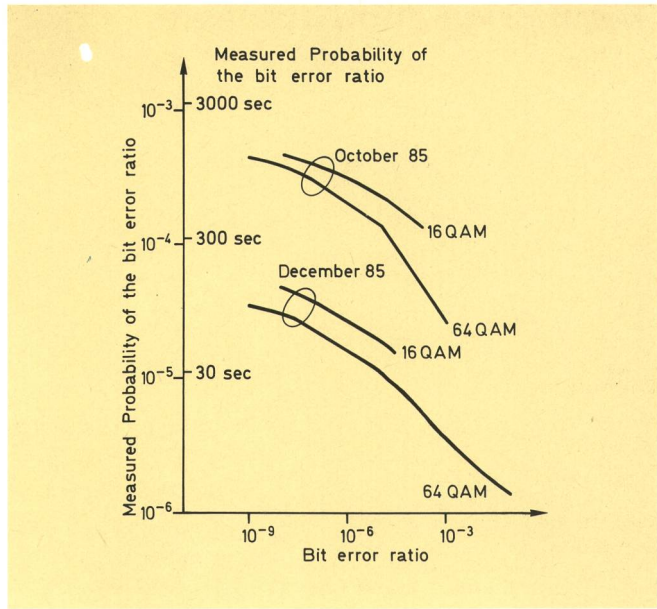


Fig. 32  
Measured cumulative distributions of the bit error ratios

## Bibliography

- [1] *Liniger M.* One Year Results of Sweep Measurements of a Radio Channel, Conference Record, IEEE International Conference on Communications (ICC'83), 1983.
- [2] *Liniger M.* More Results on the Transfer Functions of Cross-Polarized and Diversity-protected RF-Channels, International Symposium on Antennas and Propagation (ISAP'85), 1985.
- [3] *Rummler W. D.* Time- and Frequency-Domain Representation of Multipath Fading on Line-of-Sight Microwave Paths, Bell System Technical Journal 59 (1980) 5 p. 763.
- [4] *Greenstein L. J. and Czekay B. A.* A Polynomial Model for Multipath Fading Channel Responses, Bell System Technical Journal 59 (1980) 7 p. 1197.
- [5] *Anderson C. W., Barber S. and Patel R.* The Effect of selective Fading on Digital Radio, Conference Record, IEEE International Conference on Communications (ICC'78), 1978.
- [6] *Martin L.* Statistical Results on Selective Fading, Conference Record, IEEE International Conference on Communications (ICC'83), 1983.
- [7] *Gardina M. F. and Vigants A.* Measured Multipath Dispersion of Amplitude and Delay at 6 GHz in a 30 MHz Bandwidth, Conference Record, IEEE International Conference on Communications (ICC'84), 1984.